Experimental Verification of Load and Resistance Factor Inelastic Design Limits

BRYAN A. HARTNAGEL, MICHAEL G. BARKER, AND DAVID C. WEBER

More economical steel bridge designs can be realized using inelastic design provisions. However, current provisions apply only to compact steel bridges. Expanding inelastic design provisions to include noncompact sections is desirable because of the wide use of plate girders with thin webs. Previous research has shown that noncompact girders have predictable moment-rotation behavior that can be incorporated into inelastic design provisions. However, even though the analytical tools exist, large-scale testing is necessary to validate theoretical engineering practice. A report is given of the first of three composite continuous girder tests from a project with the objectives of validating current inelastic design procedures and developing new provisions for bridges comprising noncompact girders. The first girder test was a half-scale, three-span composite beam with compact sections extracted from a prototype bridge designed using inelastic procedures. The two future tests will be two-span composite beams with noncompact sections. The results of the first girder test show that current analytical techniques effectively predict the elastic and inelastic behavior of compact girders. The first test also validated the inelastic design provisions at all design limit states.

Alternate load factor design (ALFD) procedures (*1*) were adopted by AASHTO in 1986. The procedures account for the reserve strength inherent in multiple-span steel girder bridges by allowing redistribution of negative elastic moments at piers to adjacent positive moment regions. The redistribution causes slight inelastic rotation at the interior pier sections and some residual permanent deflection. After the redistribution, the structure achieves shakedown (*2*): deformations stabilize and future loads are resisted elastically.

ALFD procedures allow the designer more flexibility and the possibility of more economical designs by eliminating the need for providing cover plates and numerous flange transitions at negative moment regions (*3*). However, ALFD provisions apply only to steel beam bridges comprising compact sections. Expanding inelastic design provisions to include noncompact sections is desirable because of the wide use of plate girders with thin webs. The ALFD provisions are incorporated into the new AASHTO load and resistance factor design (LRFD) bridge design specifications (*4*).

A joint National Science Foundation, American Institute for Steel Construction, American Iron and Steel Institute, and Missouri Highway and Transportation Department project (*5*), Development and Experimental Verification of Inelastic Design Procedures for Steel Bridges Comprising Noncompact Sections, will consist of three composite, single-girder tests. Simulated moving loads in the elastic and inelastic range will be cyclically applied to the test girders. Afterward, the girders will be tested to failure. The first test consists of a three-span, compact, rolled section, whereas the other two tests will be two-span girders with typical noncompact plate girder sections. The project will verify design limit behavior of current inelastic design provisions for compact bridges and extend the inelastic procedures to include noncompact plate girder designs. This paper presents the design, modeling, and experimental results from the first three-span rolled-beam test (*6*).

Department of Civil Engineering, E2509 EBE, University of Missouri-Columbia, Columbia, Mo. 65211.

INELASTIC DESIGN OF STEEL GIRDER BRIDGES

The ALFD inelastic design procedures (*1*) specify requirements at service load levels (nominal dead load plus normal traffic), overload levels (nominal dead load plus an occasional heavy vehicle), and maximum load levels (factored dead load plus a one-time maximum vehicle). Inelastic LRFD provisions (*4*) specify these load combinations as Service I, Service II, and Strength I, respectively. The LRFD procedures also have a separate fatigue load combination. Following are the LRFD load combinations at the respective load levels:

$$\text{Fatigue—}D + 0.75L(1 + I), \quad (1a)$$
$$\text{Service I—}D + 1.00L(1 + I), \quad (1b)$$
$$\text{Service II—}D + 1.30L(1 + I), \text{ and} \quad (1c)$$
$$\text{Strength I—}1.25DC + 1.50DW + 1.75L(1 + I), \quad (1d)$$

where

D = dead load,
L = live load with lateral distribution factor,
I = impact factor (33 percent),
DC = component dead load (slab, beam, and barrier curbs), and
DW = wearing surface.

Fatigue and Service I load levels are for fatigue and live-load deflection checks. At the Service II level, after interior pier elastic moments are redistributed to adjacent positive moment regions, the design requirement or limit-state criterion is a limiting stress at positive moment regions. Finally, at the Strength I level, a mechanism must not form with the application of the factored loads.

PROTOTYPE BRIDGE DESIGN

The three-span (18.3, 23.2, and 18.3 m) (60, 76, and 60 ft), two-lane prototype bridge was designed according to the LRFD bridge design specifications using the inelastic design provisions (*4*). Four W30 × 108 rolled beam girders with a girder spacing of 3.05 m (10 ft) were used to support the 11.0-m (36-ft) wide roadway. Yield strength of the steel was 345 MPa (50 ksi). The deck was 203 mm (8 in.) thick with 27.6 MPa (4,000 psi) compressive strength concrete and Grade 60 reinforcing steel. A future wearing surface of 0.57 kPa (12 psf) [about 25 mm (1 in.) of asphalt] and barrier curbs

weighing 4.45 kN/m (305 plf) [a standard 406-mm (16-in.) concrete barrier curb] were considered as composite dead loads. The bridge was designed assuming unshored construction. Also, the LRFD HS20 design vehicle in combination with a 9.34 kN/m (640 plf) lane load was used for determining live load effects. The 1/2-scale experimental test girder models an interior girder from the bridge system. Following is a description of the design procedures used to check an interior girder from the prototype bridge (*6*).

Elastic Analysis Techniques

A prismatic elastic analysis was used to compute the noncomposite dead load moments, and elastic nonprismatic analyses were used to determine the composite dead load moments and the live load plus impact moment envelopes. LRFD lateral distribution factors were used to approximate the amount of live load applied to a single girder. According to the LRFD specifications (*4*), the lateral distribution factor is 0.77 lanes per girder for moment and 0.95 lanes per girder for shear and reactions. Figure 1 shows the total live and dead load moment envelopes for the prototype girder including impact and distribution factors.

Design Limit States

Fatigue Limit State

The LRFD provisions provide spacing requirements for shear studs on the basis of fatigue and strength limits. Stud fatigue controlled the overall fatigue requirements for this design. A total of 204 pairs of shear studs 25 mm (1 in.) in diameter by 127 mm (5 in.) in length were spaced at 305 mm (12 in.) on center along the girder, except for a spacing of 152 mm (6 in.) on center at the end supports.

Service I Deflection Limit State

LRFD live-load deflection criteria for slab-on-girder bridges are subject to designer discretion (*4*). However, LRFD provisions do allow the use of past practice for deflection control. The current deflection limit (*7*) suggested by AASHTO is equal to the span length L, in feet, divided by 800 for bridges with no pedestrian traffic. The controlling design deflection resulted from two loaded lanes of the design truck plus impact. Assuming equal distribution of load to all the girders, a distribution factor of two lanes/four girders = 0.5, along with an elastic nonprismatic analysis, was used to calculate the maximum live load plus impact deflection of 30 mm (1.18 in.). The suggested AASHTO deflection limit is calculated as 76 ft × 12 in./800 = 1.14 in. or 29 mm for the prototype.

Service II Limit State

The Service II check ensures that the nominal dead load plus occasional overload vehicles equal to $1.30L(1 + I)$ will not cause excessive deformations. Elastic overload moments are redistributed because of inelastic pier rotations, θ, caused by localized yielding at the pier. The pier sections resist bending according to the following relationship (*4*):

$$M = M_P[0.7 - 60.0(\theta)] \leq 1.0 \qquad (2)$$

where $-0.008 \leq \theta \leq 0$ radians, and

M = LRFD moment rotation curve for pier sections,
θ = inelastic rotation at pier in radians (negative), and
M_P = section plastic moment capacity.

Residual moments that remain in the beam after the load is removed can be related to the pier rotation through an inelastic conjugate beam analysis developed by Dishongh (*8*). The moments at the piers, M_a and M_b, and the residual moment are

$$M_a = \frac{\frac{EI\theta_i}{L}}{\left[-\frac{A}{3} - \frac{1}{2} + \frac{\frac{B}{6} + \frac{1}{4}}{B+1}\right]} \qquad M_b = \frac{-M_a}{2B+2}$$

$$M_R = M_a + M_b \qquad (3a, 3b, 3c)$$

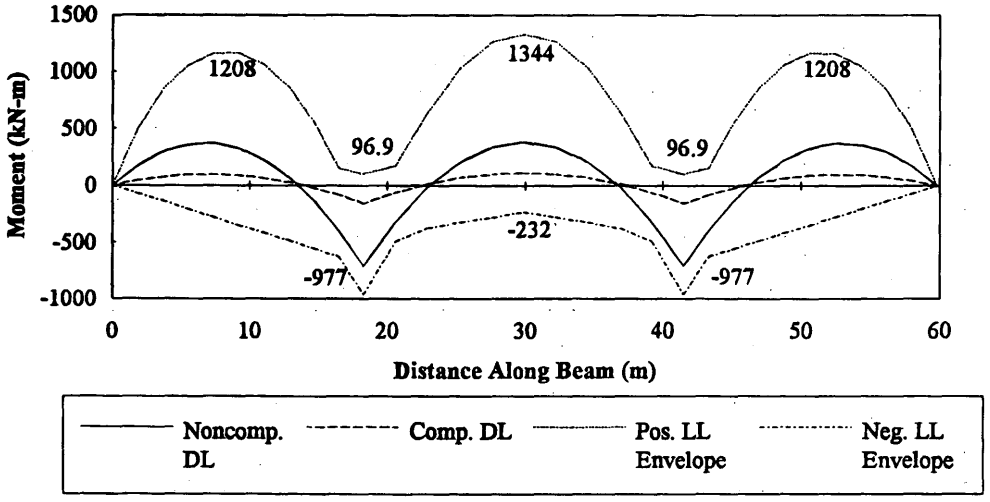

FIGURE 1 Moment envelopes for the prototype girder.

where A and B are ratios of the two outer-span lengths to the center-span length equal to 18.3/23.2 = 0.79. At the pier section, the applied Service II moment [$D + 1.30L(1 + I)$] (Equation 1c), plus the residual moment (Equation 3c) is equal to the actual moment defined by the moment rotation relationship (Equation 2) for the pier sections:

$$[D + 1.30L(1 + I)] + M_R = M_P[0.7 - 60(\theta)] \quad (4)$$

Solving Equation 4 for the plastic rotation at the pier section yields $\theta = -0.00083$ radians. The residual moment was computed to be M_R = 46 kN-m (34 kip-ft) at the two pier sections and throughout the middle span and linearly decreased to 0 at the end supports. The residual moment field is symmetric because of the symmetry of the bridge design.

At the Service II load level, centerline stresses in the center span were found to be maximum. LRFD states that the applied stresses must be less than or equal to 0.95 of the flange yield stress, F_y, for a composite section in positive bending. The maximum Service II stress is determined by superposition of stresses where the live load moment stress component is equal to the elastic moment plus the redistributed residual moment. The total stress was calculated as 330 MPa (47.9 ksi), which is approximately equal to the requirement of 0.95 F_y = 327 MPa (47.5 ksi).

Strength I Limit State

To satisfy the ultimate strength requirement, a plastic collapse mechanism must not form with the application of Strength I factored loads. LRFD inelastic provisions use an effective plastic moment, M_{PE}, at the negative moment pier hinge sections. The effective plastic moment ensures adequate inelastic rotation capacity at rotating hinges. The mechanism check was carried out by applying the factored dead loads [$1.25DC + 1.50DW$], moving the factored design truck [$1.75L(1 + I)$] over the entire beam in tenth-point increments, and calculating the plastic collapse load factors for all truck positions (*9*). The critical mechanism, using M_{PE} at the pier sections, was the maximum positive center-span loading configuration. The plastic collapse load factor was found to be 1.38. The structure can withstand 38 percent more factored live loads than is caused by the Strength I factored design live loads. Thus, Strength I requirements did not control the design.

Summary of Design Limits

The Service I level maximum live-load deflection was 30 mm (1.18 in.). The Service II limit state was the controlling design limit with a maximum centerline stress of 330 MPa (47.9 ksi) versus an allowable stress of 327 MPa (47.5 ksi). Strength I loads did not control the design of the prototype; the theoretical collapse capacity is 38 percent higher than the Strength I factored loads.

TEST GIRDER MODEL DESIGN

The test girder was a scaled interior girder extracted from the prototype bridge. Structural modeling techniques were employed to determine the theoretical scale factors, S, for the fundamental measures of interest in the 1/2 scale model. Steel and concrete properties for the prototype and the model were identical; therefore, the independent variables were chosen as elastic modulus E (S_E = 1) and length L (S_L = 2). A half-scale model of the deck effective width, deck thickness, deck reinforcement, shear studs, and bearing stiffeners was easily produced. However, an exact half-scale model of the W30 × 108 rolled shape did not exist so a W14 × 26 was chosen as the best alternative. Because of this choice, the actual scale factors for several fundamental measures did not match the theoretical scale factors. A summary of important cross-sectional properties is presented in Table 1, along with the theoretical and actual scale factors of these properties. In Table 1

- I^+ = positive bending section moment of inertia in positive moment regions,
- I^- = negative bending section moment of inertia in negative moment regions,

TABLE 1 Prototype and Model Girder Properties

Item	Prototype	Model	P/M = S_{actual}	P/M = S_{theory}
$I^+_{LL,COMP}$ (10^6mm^4)	5,620	313	17.96	16
$I^+_{DL,COMP}$ (10^6mm^4)	4,330	241	17.97	16
$I^-_{DL\&LL,COMP}$ (10^6mm^4)	2,900	158	18.35	16
I_{STEEL} (10^6mm^4)	1,860	102	18.24	16
$S_x{}^+_{LL,COMP}$ (10^3mm^3)	7,560	891	8.48	8
$S_x{}^+_{DL,COMP}$ (10^3mm^3)	6,920	815	8.49	8
$S_x{}^-_{DL\&LL,COMP}$ (10^3mm^3)	5,940	698	8.51	8
S_{xSTEEL} (10^3mm^3)	4,910	578	8.49	8
$b_f / 2t_f$	6.9	6.0	1.15	1
d / t_w	54.7	54.5	1.00	1
$M_P{}^+_{COMP}$ (kN-m)	3,680	428	8.60	8
$M_P{}^-_{COMP}$ (kN-m)	2,810	316	8.89	8
$M_{PE}{}^-_{COMP}$ (kN-m)	2,250	252	8.93	8

10^6mm^4 = 2.4025 in^4; 10^3mm^3 = 61.024 10^{-3}in^3; 1 kN-m = 0.7368 kip-ft

$COMP$ = composite section (steel + rebar for I^-)
S_x = section modulus,
S_{actual} = P/M = actual scale factor (prototype/model scale factor),
S_{theory} = P/M = theoretical scale factor (prototype/model scale factor),
b_f = width of flange,
t_f = thickness of flange,
d = section depth, and
t_w = thickness of web.

Loading applied to the model was scaled to simulate equal stresses in the model and the prototype. Because scale factors for all the section moduli were approximately 8.5, as shown by the shaded portion of Table 1, to model equal stresses, all prototype bending moments were factored by 1/8.5. Also shown in Table 1 are scale factors computed for the plastic moment capacities at the critical sections.

Compensatory dead load was added to accurately simulate dead load stresses because a half-scale model weighs only one-quarter of the prototype. Ten concrete blocks weighing 8.9 kN (2,000 lb) were hung from the bottom of the W-shape before the concrete deck was placed to compensate for the self-weight lost because of scaling. Additional concrete blocks were placed on top of the deck after it hardened to represent the composite dead loads (wearing surface, guard rails, etc.).

Moving live loads were simulated with four discrete loading points on the test beam, as indicated in Figure 2 (P1 and P2 shown on figure; P3 and P4 symmetric). Influence lines for each of the four loading points were used to determine the sequence of loads needed to simulate a moving truck. The total moment envelope produced by the four discrete loading points is shown in Figure 3 along with the scaled theoretical design truck [$L(1+I)$] moment envelopes. The truck load sequence could be linearly adjusted to represent any percentage of the modeled truck design weight (LL).

Several different measurements were recorded for the test, including deck slip, rotation, deflection, reaction, and strain gauge readings. Dial gauges were used to measure deflections. An 890-kN (200-kip) compression load cell was placed under each support to measure the reactions of the beam. The locations of these measurements are shown in Figure 2.

TEST SEQUENCE

The modeled live loads were applied to the test beam cyclically at various load levels. The following design load levels and collapse loads were examined rigorously because of their importance:

1. Service I,
2. Service II,
3. Strength I, and
4. Plastic collapse load (Strength I loads proportionally increased until failure).

The entire loading history of the test is as follows. Elastic low-level tests were carried out at 10, 20, 40, 60, 70, 80, and 90 percent LL. These provided an opportunity to confirm elastic behavior and

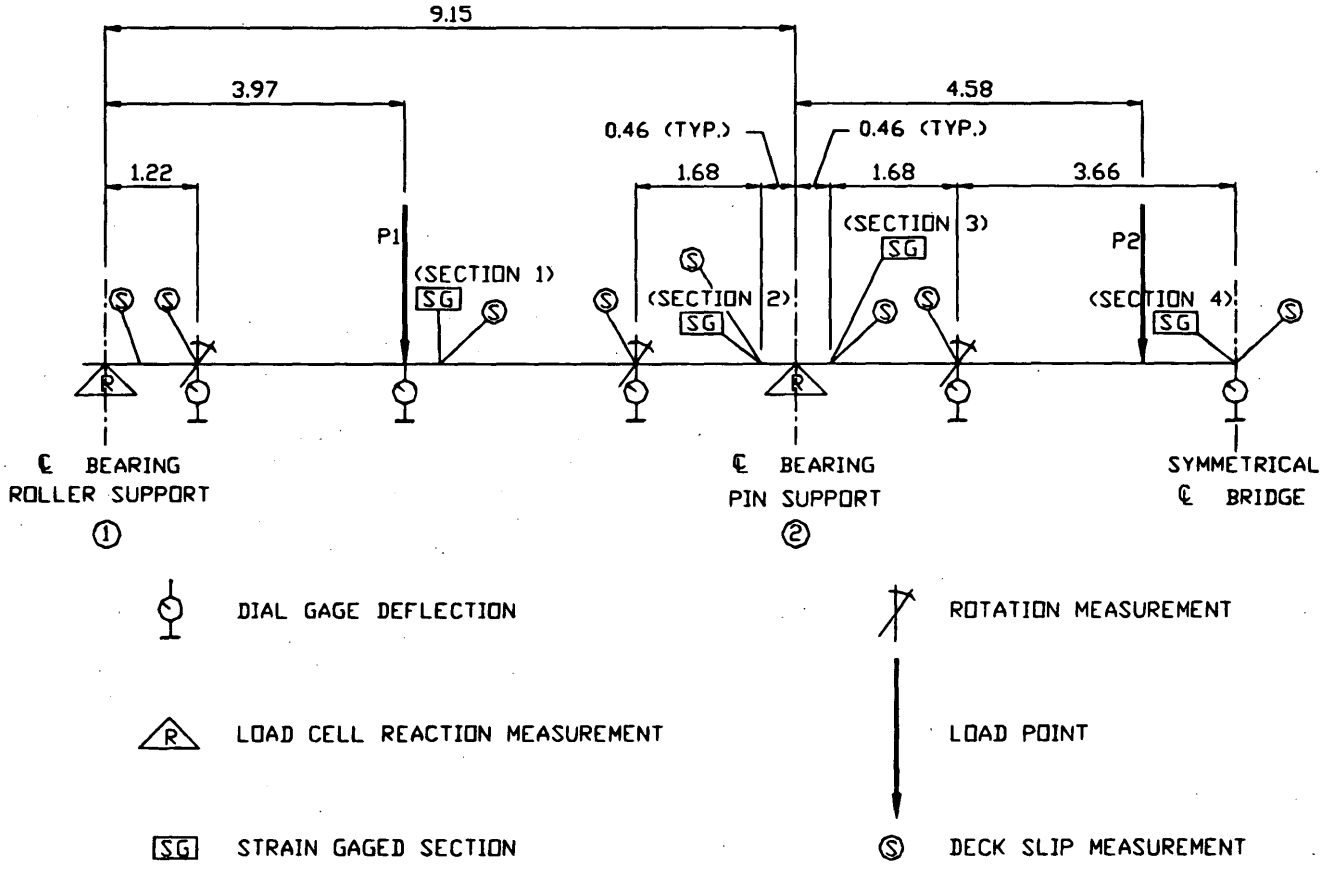

FIGURE 2 Measurement and load locations.

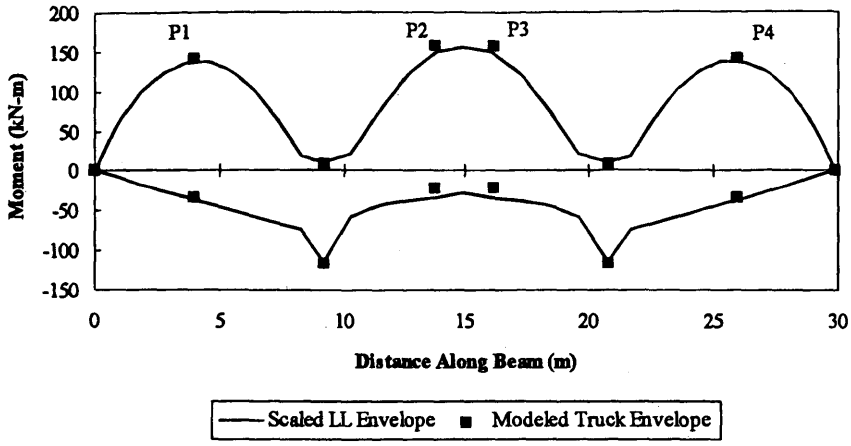

FIGURE 3 Modeled truck moment envelope.

instrumentation performance. Service I level live loads (100 percent LL) were applied to examine fatigue (ratioed to 75 percent LL) and deflection requirements of the LRFD provisions. Increasing the loads toward the Service II level, live loads of 110 and 120 percent LL were applied to examine the behavior in this range of loads.

At the Service II live-load level (130 percent LL), the girder experienced controlled inelastic behavior. After seven cycles, deflections stabilized and the girder behaved elastically for additional cycles. The inelastic behavior is characterized by residual deflection or permanent set. Design provisions predict this residual deflection and limit stresses in positive moment portions of the structure to control the amount of permanent set. Live loads were applied at 140, 155, and 166 percent LL to examine the inelastic behavior above the Service II level. The last simulated moving load test was at 175 percent LL plus factored dead loads. This loading represents the worst possible maximum design load level applied to a bridge.

After the cyclic tests, the girder was tested to failure by monotonically increasing loads proportioned to represent the theoretical design collapse configuration. This configuration simulated a stationary truck where the center axle of the truck was located at the centerline of the middle span. The additional factored dead load was applied by adding extra simulated loads to the P1 through P4 discrete load locations.

DESIGN LIMIT TEST RESULTS

Service I Level Behavior

The main design concerns at the Service I load level are fatigue and live-load deflection control. Fatigue stress criteria limited the allowable fatigue stress range to 40 MPa (5.8 ksi); the corresponding strain is 200 με. Strains (ratioed to 75 percent LL) at the top flange of Sections 1 and 2 (Figure 2) were 71 and 158 με, respectively. Thus, the model met the Category C fatigue stress requirement.

There was 1.9 mm (0.08 in.) of permanent set measured at the bridge centerline before applying the 100 percent LL sequence. After four 100 percent LL cycles, residual deflection at the center of the bridge was 3.1 mm (0.12 in.). The largest live load deflection at 100 percent LL occurred in the middle span (with P2 and P3 loaded) and was measured as 31.0 mm (1.22 in.). Theoretical deflection of the model was computed as 29.5 mm (1.16 in.) using a nonprismatic analysis and the actual loads at P2 and P3. This indicates that the model represented effectively the prototype bridge live-load deflection behavior.

Service II Level Behavior

As the load level was increased to 130 percent LL, strain measurements at negative bending sections were substantially higher than the theoretical elastic strains, indicating that some yielding had occurred. LRFD provisions require that the stresses in positive bending regions be less than 0.95 F_y after redistribution of moments. A maximum strain of 1449 με occurred at Section 4. The maximum strain allowed by LRFD for 345 MPa (50 ksi) steel is 0.95 × 1724 με = 1,638 με. Therefore, the structure met the Service II limit-state criterion.

A permanent set of 9.6 mm (0.38 in.) occurred at Section 4 after seven 130 percent LL cycles. Theoretical residual deflections at the Service II level can be calculated from the prototype design residual moments and rotations, 46 kN-m (34 kip-ft) and 0.00083 radians, respectively, previously determined using the LRFD pier moment-inelastic rotation curve. Two theoretical prototype residual deflections were calculated using the conjugate beam analogy (*6*). The first used a prismatic beam with a weighted average for the moment of inertia and found the scaled residual deflection to be 3.3 mm (0.13 in.). Another method used a nonprismatic beam with a reduced moment of inertia for 20 percent of the span on each side of the interior piers. The second method yielded a scaled residual deflection of 6.6 mm (0.26 in.). The 9.6-mm (0.38-in.) actual residual deflection was nearly three times the scaled theoretical value of (6.55/2) = 3.3 mm (0.13 in.). Calculated residual deflections did not reflect the measured values because the LRFD pier moment-inelastic rotation curve apparently does not describe the observed softer behavior of the model pier section (*6*). Residual deflections were also computed using a softer pier moment-inelastic rotation curve presented in the unified autostress method (UAM) developed by Schilling (*10*). The softer UAM pier moment-inelastic rotation curve produced a higher residual moment and inelastic rotation [132 kN-m (97 kip-ft) and 0.0024 radians]. Again, two residual deflections were computed using the conjugate beam analogy. These residual deflections were 9.1 mm (0.36 in.) and 18.3 mm

(0.72 in.) for the prismatic averaged inertia and the nonprismatic analysis, respectively. Therefore, the 9.6-mm (0.38-in.) measured residual deflection corresponds well with the scaled value calculated using the softer pier moment-rotation relationship of (18.31/2) = 9.2 mm (0.36 in.).

Strength I Level Behavior

The Strength I mechanism test was conducted by first applying the simulated factored portion of the dead load to P1, P2, P3, and P4. Live loads were then applied to P1, P2, and P3 to recreate the prototype mechanism moment diagram. The P1 and P4 loads were set to load control for the duration of the collapse test while the P2 and P3 loads were slowly increased under stroke control until the girder failed by concrete crushing. Figure 4 is the total load at P2 and P3 (P2 + P3) plotted against the deflection at the girder centerline. The figure shows the Strength I factored load level in relation to the load-deflection response. The figure clearly shows that the girder had excess capacity (36 percent) beyond the Strength I loading in accordance with the design calculations.

SHAKEDOWN BEHAVIOR

Each modeled truck weight level percentage loading was repeated until the residual deflections stabilized and the bridge experienced shakedown. Figure 5 shows the residual deflection at the centerline of the bridge in terms of the percent live load level. This shakedown plot shows how the structure experienced increasing permanent set as the live load level increased. The onset of permanent set occurred at 70 percent LL. After the last cycle of loads, the girder had a residual deflection at the centerline of 65 mm (2.56 in.).

Stabilization of residual deflections was achieved at all live load levels except for the 175 percent LL level. The 175 percent LL level was somewhat different from that of other load sequences because it included extra loads to simulate the factored portion of the dead load. The 175 percent LL level was actually the Strength I load level as defined by the LRFD provisions.

Three cycles were carried out at the Strength I load level; each cycle resulted in large increases in residual deflection. The cyclic live loading portion of the test concluded at this level because some slight web buckling at the pier sections was detected. At the Strength I load level, the structure may or may not have shaken down, so this level was not necessarily the incremental collapse load. However, it can be concluded that the incremental collapse load occurred above the 166 percent LL level.

Figure 6 shows the percent of modeled truck weight versus deflection relationship for the outer span of the model structure. The theoretical elastic deflections were calculated with an elastic nonprismatic analysis of the structure under the modeled loads applied at location P1. This figure indicates that after the 120 percent LL cycle, this portion of the structure begins to behave nonlinearly. The percent of modeled truck weight versus deflection relationship for the middle span of the test bridge (for P2 and P3 loaded) is shown in Figure 7. The middle span portion of the specimen began to behave nonlinearly at the 70 percent LL cycle.

PLASTIC COLLAPSE BEHAVIOR

The theoretical plastic collapse load was calculated using the effective plastic moment at the pier sections and the plastic moment capacity of the section at location P2. As indicated in Figure 4, the experimental plastic collapse capacity exceeded the Strength I load level by 36 percent, which was consistent with the design. The actual collapse load was within 1 percent of the theoretical collapse load.

After sustaining about 356 mm (14 in.) of deflection at the bridge centerline [in addition to the 65 mm (2.56 in.) from the shakedown tests], the concrete crushed at the bridge centerline. This deflection (length/deflection = 33) illustrates that this compact girder had tremendous ductility. Once the concrete crushed, the load was removed from the specimen. Over 51 mm (2 in.) of elastic deflection was recovered during unloading.

SUMMARY AND CONCLUSIONS

More economical steel bridge designs (for compact girders) can be realized using inelastic design provisions. Inelastic design provisions can reduce material and fabrication costs by eliminating the

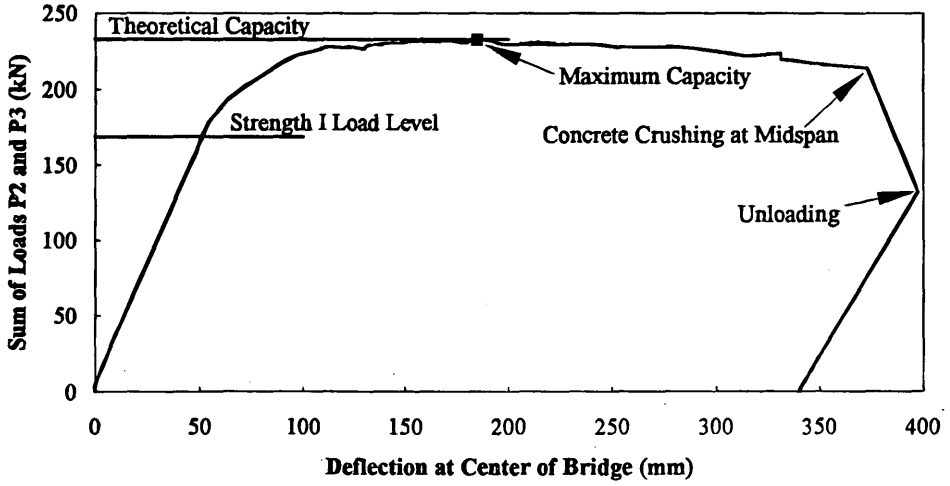

FIGURE 4 Collapse test middle span load: deflection response.

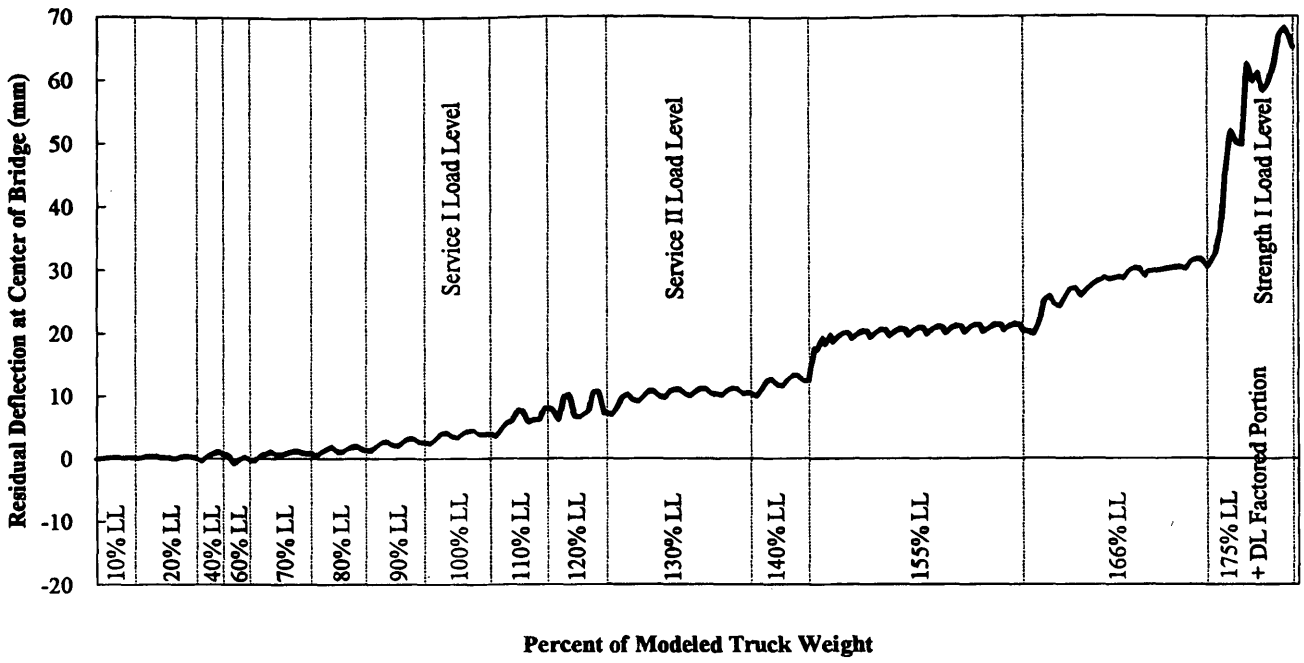

FIGURE 5 Residual deflection versus percent of modeled truck weight.

need for numerous flange transitions and cover plates at interior piers (*3*). Bridge safety is not compromised because, after the structure has experienced several passes of the design limit loads, future loads are resisted elastically. Results from this test validate the LRFD inelastic provisions at all design limit states. Extending provisions to allow inelastic design for bridges comprising noncompact sections would also be beneficial. However, even though the analytical tools exist (*8*) for developing inelastic design procedures for these girders, large-scale testing is necessary to validate theoretical engineering practice.

The test results reported herein give an overview of the general elastic, inelastic, and plastic behavior of a 1/2-scale three-span composite compact test beam. The experimental results compared well with theoretical expectations. However, the LRFD inelastic design provisions significantly underestimated the measured Service II load level (130 percent LL) residual deflections. For inelastic design, this permanent set could be included in the camber with the dead load deflections. Using other behavior models, the residual deflection was more accurately estimated. Future analysis of this test and others will yield insight into the best approach for estimating these deflections.

The plastic collapse test illustrated the available ductility in compact composite beams. The measured collapse load was within 1 percent of the predicted ultimate capacity. The primary reason that the beam behaved so well is that it is compact with the flanges being well below the compactness requirements (ultracompact) (*10*). In the next two girder tests planned for this project, the flanges will still be ultracompact, but the webs will have typical ratios of plate girder

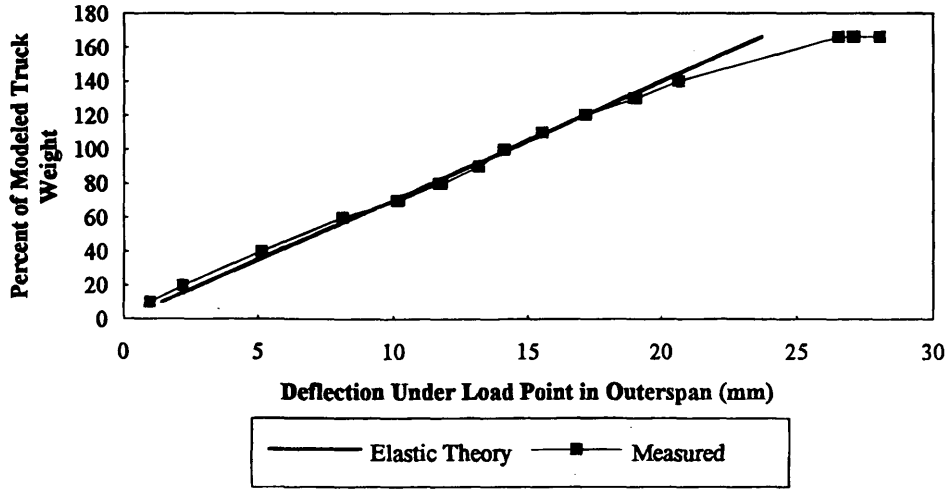

FIGURE 6 Outer span percent of modeled truck weight: deflection response.

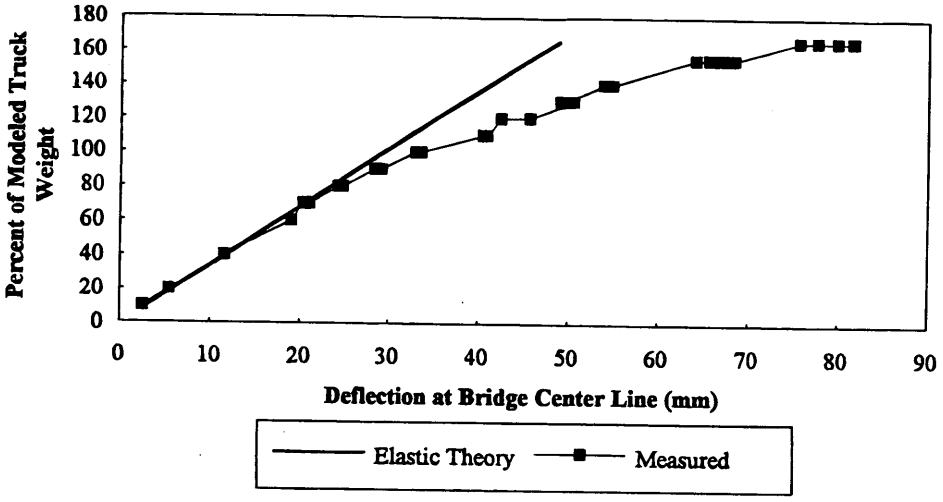

FIGURE 7 Middle span percent of modeled truck weight: deflection response.

width to thickness. However, previous work has shown that, although these girders are not as ductile, the noncompact sections have predictable moment-rotation behavior (*8*) that can be incorporated into inelastic design provisions. The second two noncompact girder tests from this project will provide vital information for the development of inelastic design provisions for noncompact girders.

ACKNOWLEDGMENTS

The authors gratefully acknowledge the sponsors of this work: the National Science Foundation, the American Iron and Steel Institute, the American Institute for Steel Construction, the Missouri Highway and Transportation Department, Louisiana Transportation Research Center, Bethlehem Steel, Nucor-Yamato Steel, U.S. Steel, St. Louis Screw & Bolt Co., and Stupp Bros. Inc.

REFERENCES

1. *Guide Specification for Alternate Load-Factor Design Procedures for Steel Beam Bridges Using Braced Compact Sections.* AASHTO, Washington, D.C., 1986.
2. Neal, B. G. *The Plastic Methods of Structural Analysis.* John Wiley & Sons, 1956.
3. Barker, M. G. Inelastic Design and Rating of Steel Girder Bridges Proc., *1993 National Symposium on Steel Bridge Construction,* Atlanta, Nov. 1993, pp 2.1–2.17.
4. *AASHTO LRFD Bridge Design Specifications.* AASHTO, Washington, D.C., 1994.
5. Barker, M. G. *Development and Experimental Verification of Inelastic Design Procedures for Steel Bridges Comprising Noncompact Sections.* National Science Foundation, Washington, D.C., 1993–1996.
6. Weber, D. C., *Experimental Verification of Inelastic Load and Resistance Factor Design Limits.* Thesis. University of Missouri—Columbia, Aug. 1994.
7. *Standard Specification for Highway Bridges.* AASHTO, Washington, D.C., 1992.
8. Dishongh, B. E. *Residual Damage Analysis: A Method for the Inelastic Rating of Steel Girder Bridges.* Thesis. University of Minnesota, Minneapolis, June 1990.
9. Barker, M. G., and T. V. Galambos. Shakedown Limit State of Compact Steel Girder Bridges. *Journal of Structural Engineering,* ASCE, Vol. 118, No. 4, April 1992, pp. 986–998.
10. Schilling, C. G. A Unified Autostress Method. *Development of Design Specifications for Continuous Plate-Girder Bridges.* Project 51. American Iron and Steel Institute, 1989.

Publication of this paper sponsored by Committee on Steel Bridges.